Electronic Supplementary Material (ESI) for Inorganic Chemistry Frontiers.

Supplementary Information

Low temperature water-assisted crystallization approach to MOF@TiO_2 core-shell nanostructures for efficient dye removal

Shouxin Bao, [a,b,‡] Mingyang Lv, [a,‡] Chen Zhao, [c] Ping She, [c] Zhenyu Lei, [c] Xiaowei Song [a,*] and Mingjun Jia [c,*]

[a] State Key Laboratory of Inorganic Synthesis and Preparative Chemistry, College of Chemistry, Jilin University, Changchun 130012, P. R. China.

[b] State Key Laboratory of Radiation Medicine and Protection, School for Radiological and Interdisciplinary Sciences (RAD-X) & Collaborative Innovation Center of Radiation Medicine of Jiangsu Higher Education Institutions, Soochow University, Suzhou 215123, P. R. China.

[c] Key Laboratory of Surface and Interface Chemistry of Jilin Province, College of Chemistry, Jilin University, Changchun 130012, P. R. China.

Corresponding authors: xiaoweisong@jlu.edu.cn (X. Song), jiamj@jlu.edu.cn (M. Jia).

‡ These authors contributed equally to this work.

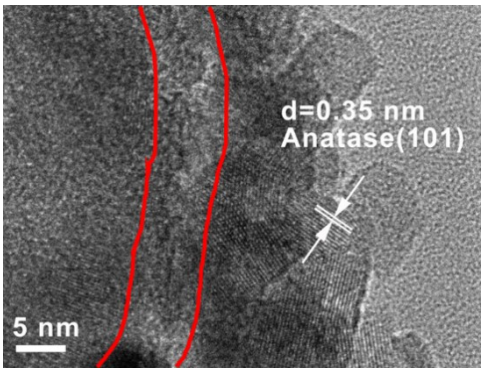

Fig. S1 HRTEM image of the interface of the MOF core and TiO_2 shell in MOF@TiO_2-A.

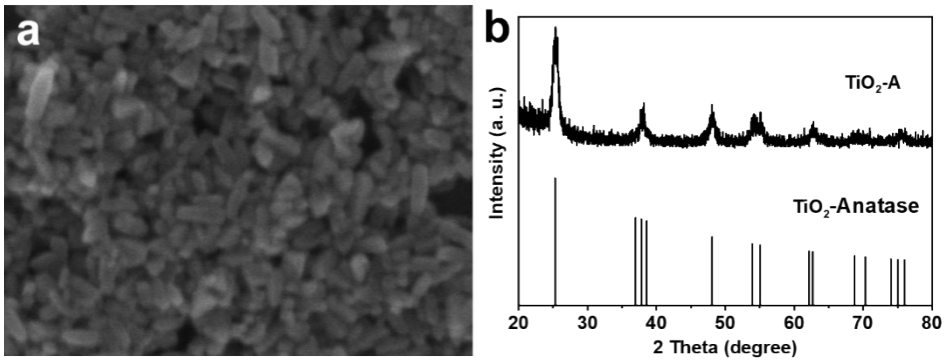

Fig. S2 SEM image (a) and PXRD pattern (b) of the as prepared TiO_2-A.

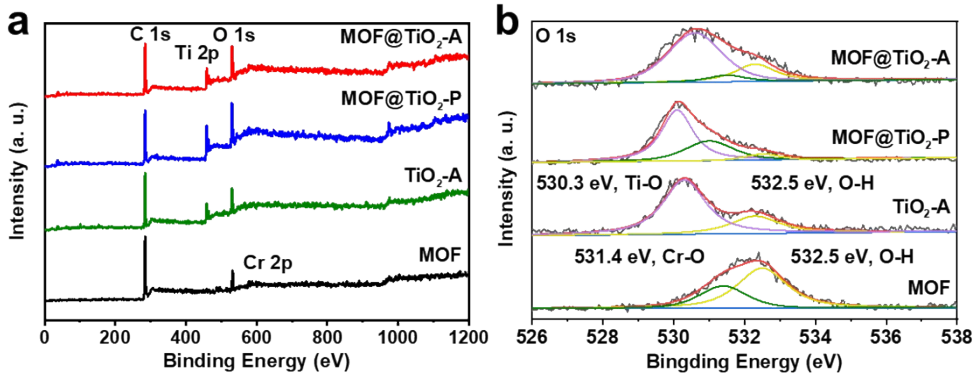

Fig. S3 XPS survey spectra (a) and O 1s XPS spectra of MOF, TiO_2-A, MOF@TiO_2-P and MOF@TiO_2-A (b).

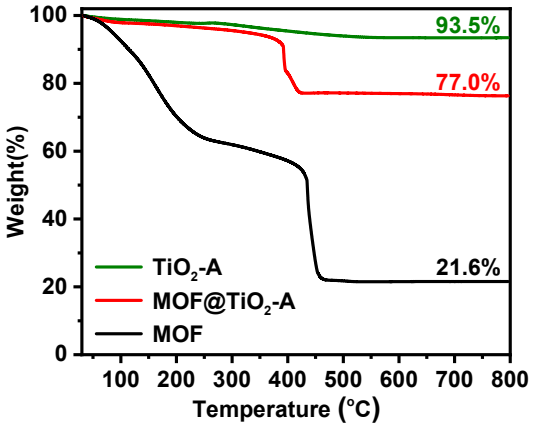

Fig. S4 TG curves of MOF, TiO_2-A and MOF@TiO_2-A.

The mass percentages of MOF and TiO_2 components in MOF@TiO_2-A are assumed to be x and 1-x. Equation below is obtained according to the remained weights of MOF, TiO_2-A and MOF@TiO_2-A.

21.6%x + 93.5% (1-x) = 77.0%

x is equal to 23% by solving this equation. That is, the mass percentages of MOF and TiO_2 components in MOF@TiO_2-A are 23 wt% and 77 wt%, respectively. This result is in consistent with that determined by ICP result (26% and 74%), which can be calculated according to the Cr:Ti molar ratio (1:11.5) and the molecular weight of MIL-101 ($Cr_3OH(H_2O)_2O[(C_6H_4)$-$(CO_2)_2]_3 \cdot 15H_2O$, 987 g mol^{-1}) and TiO_2.

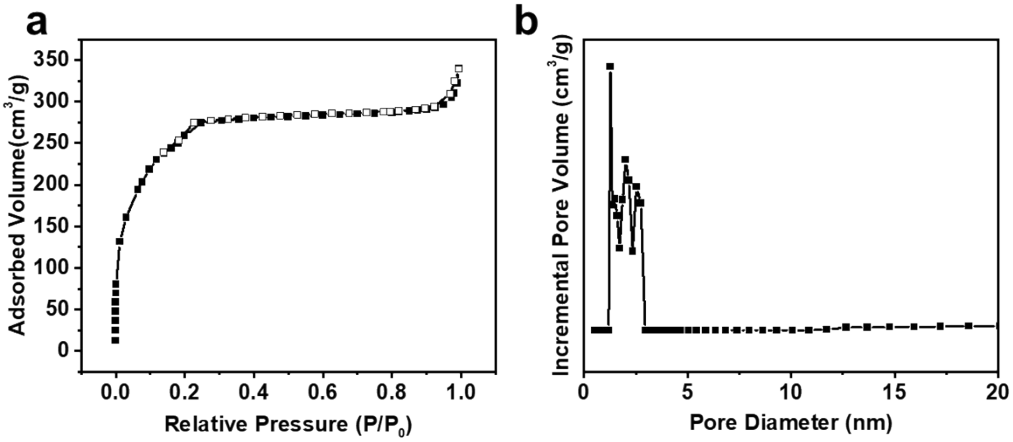

Fig. S5 Nitrogen adsorption-desorption isotherms (a), and pore size distribution curves (b) of MOF@TiO_2-P.

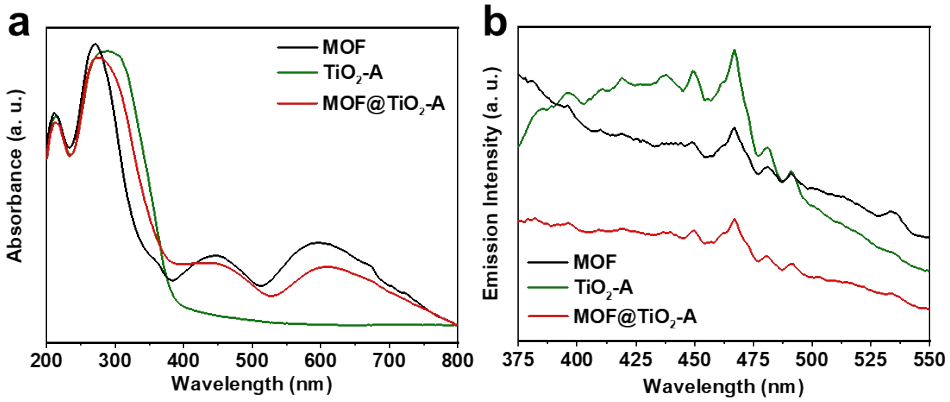

Fig. S6 UV–vis DRS (a) and PL spectra of MOF, TiO_2-A and MOF@TiO_2-A with 300 nm excitation.

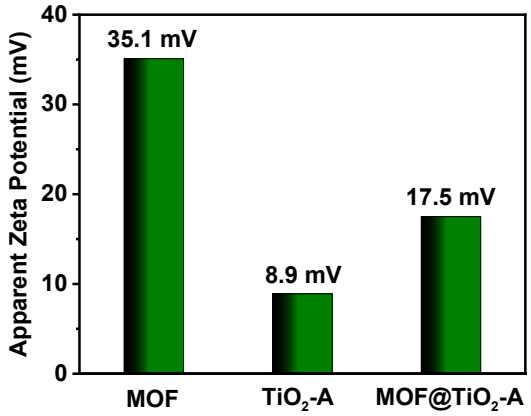

Fig. S7 Zeta potential of MOF, TiO_2-A, and MOF@TiO_2-A.

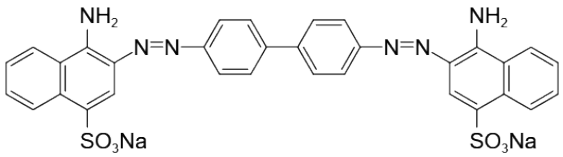

Fig. S8 Molecular structure of CR.

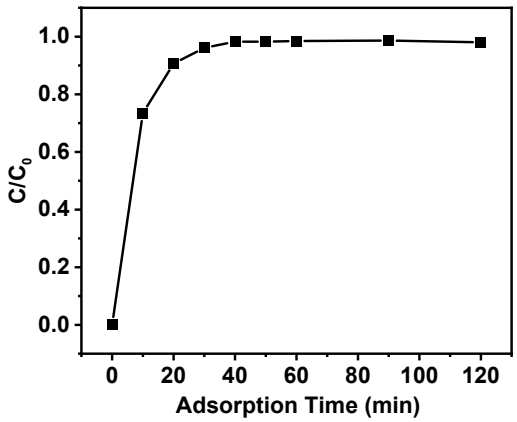

Fig. S9 Time-dependent adsorption study of MOF@TiO_2-A.

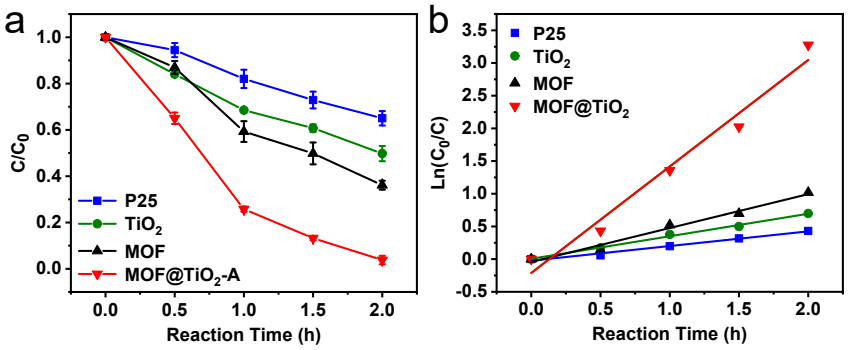

Fig. S10 Photocatalytic degradation of CR (a) and kinetic study of the degradation process (b).

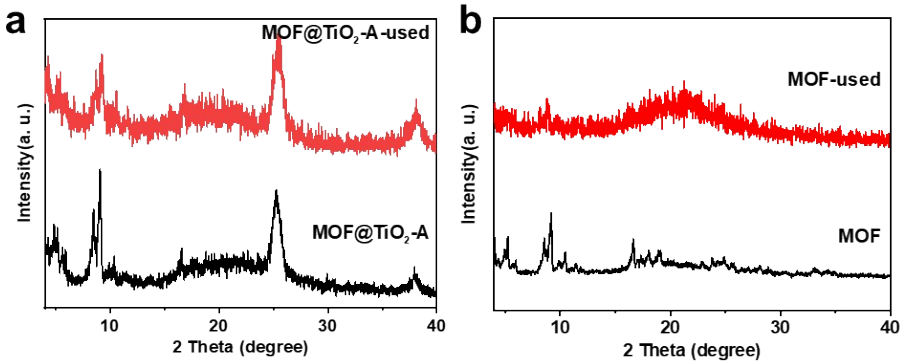

Fig. S11 PXRD patterns of fresh and used MOF@TiO_2-A (a) and MOF (b).

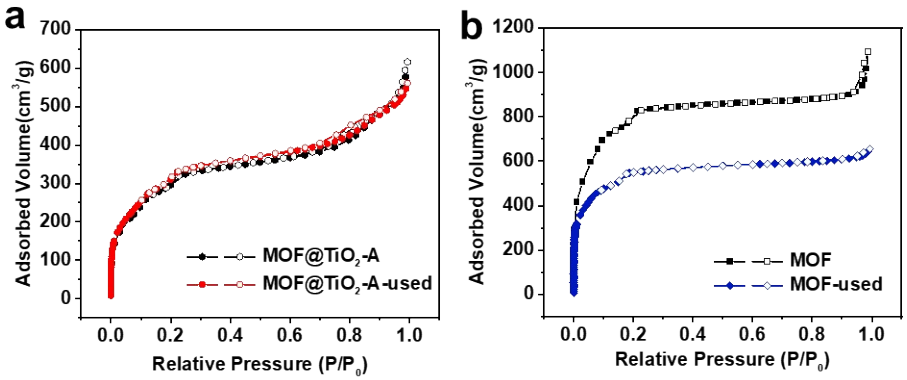

Fig. S12 Nitrogen adsorption-desorption isotherms of fresh and used MOF@TiO_2-A (a) and MOF (b).

Table S1 BET surface and pore volume of fresh and used MOF@TiO_2-A.

Sample	S_{BET} (m^2/g)			V_{total} (cm^3/g)		
	before	after	decreased	before	after	decreased
MOF@-TiO_2-A	1116	1110	0.5%	0.95	0.87	8.4%
MOF	2823	1682	40.4%	1.69	1.02	39.6%